J Mater Sci: Mater Electron **(2025) 36:10**

Cellulose-based encapsulation for all-printed flexible thermoelectric touch detectors

Joana Figueira[1,*], Mariana Peixoto[2], Cristina Gaspar[2,*], Joana Loureiro[1], Rodrigo Martins[1], Emanuel Carlos[1], and Luís Pereira[1,2]

[1] *CENIMAT|i3N, Department of Materials Science, School of Science and Technology, NOVA University Lisbon and CEMOP/UNINOVA, Caparica, Portugal*
[2] *AlmaScience, Colab, Madan Parque, Caparica, Portugal*

Received: 13 September 2024
Accepted: 9 December 2024
Published online: 20 December 2024

© The Author(s), 2024

ABSTRACT

Printed and flexible electronics have gained considerable scientific attention in recent years, driving the demand for low-energy production techniques, eco-friendly materials and flexible substrates. However, effective encapsulation is essential to protect these devices in harsh environmental conditions. Thus, sustainable encapsulant materials are critical for advancing flexible electronics. In this work, we studied three encapsulant materials—commercial plastic, polyvinyl alcohol and ethyl cellulose—applied to thermoelectric touch sensors printed on paper and fabric substrates. Ethyl cellulose demonstrated promising properties in terms of flexibility, water resistance and transparency, along with a low carbon footprint. Encapsulated substrates with ethyl cellulose exhibited high contact angles (121° on fabric and 116° on paper), indicating robust water repellency. Thermal stability tests showed minimal mass loss (10%) at 315 °C, confirming its temperature resilience. Furthermore, sensors encapsulated with ethyl cellulose retained their electric performance after water submersion for 1 min and withstood 100 bending cycles, maintaining response times below 1 s and signal output around 100 μV. These findings highlight ethyl cellulose as a viable green encapsulant material compatible with large-scale sustainable electronics manufacturing.

1 Introduction

Devices produced on a laboratory scale typically operate under fixed and controlled conditions, such as temperature (T) or humidity. In contrast, in real-world applications, these devices will face different and variable environmental conditions, along with mechanical stresses, which may compromise their performance. Many studies do not specify these highly relevant circumstances for evaluating the viability of the devices in some applications. The encapsulation step aims to protect devices under extreme conditions and meet the different usage requirements, while minimizing performance degradation. Factors such

Joana Figueira and Mariana Peixoto are co-first authors.

Address correspondence to E-mail: joanarsfigueira@gmail.com; cristina.gaspar@almascience.pt

https://doi.org/10.1007/s10854-024-14064-4

as lifetime, durability, variability and stability, are practical considerations that are seldom considered [1]. Some printed electronic devices must have selective permeability, such as ozone sensors that should be able to adsorb oxygen [2] or humidity sensors that must interact with water molecules [3, 4]. On the other hand, optical sensors typically just require a transparent or optically neutral encapsulation [5, 6]. Lastly, certain sensor types require an encapsulation to protect against the environmental abrasion and wear.

Printed electronics utilize low-energy demanding processes, such as additive manufacturing techniques, without the need for vacuum or high temperature steps. Functional inks are formulated accordingly to the desired features, and through techniques like screen-printing, inkjet printing, film casting or flexography printing, it is possible to achieve printed films on paper, fabrics, or other flexible substrates. The combination of these inks and printing methods have been used to produce different kinds of sensors, namely, for ultraviolet radiation [2, 7], mechanical pressure [8, 9], humidity [3, 10], or temperature [11]–[13]. Nonetheless, one of the most important requirements in bringing these devices to market is their encapsulation since many of the materials used in printed and flexible electronics are sensitive to oxygen or moisture [14], for instance, leading to performance losses over time. Encapsulation is also a key aspect in improving the robustness of flexible devices against mechanical impacts or bending/twisting, increasing their durability and shelf-life [15]. Encapsulation technologies have evolved from traditional rigid cover plate encapsulation, rigid inorganic film encapsulation, to the current flexible thin-film encapsulation [16], typically polymer-based materials. The commonly used materials such as parylene [17, 18], polydimethylsiloxane (PDMS) [5, 19, 20], laminated plastic [18, 21] and polyvinyl alcohol (PVA) [22, 23], among others, usually are toxic or difficult to recycle.

In this work, we explored three different encapsulant materials for flexible and screen-printed thermoelectric (TE) touch detectors on paper and fabric substrates, developed in a previous study [12]. These graphite-based thermal sensors operate based on the thermal gradient formed between the finger and the device, generating an electrical signal through the Seebeck effect. The Seebeck coefficient (S) of graphite is reported to be p-type, with positive values and relatively small magnitudes (typically bellow 30 μV/K) [11, 12, 24, 25]. However, there are ways to optimize sensor performance, including connecting multiple TE elements in series or use graphite in composites [12, 26–28]. Besides being flexible and lightweight, these touch detectors offer good performance for both naked and glove-covered skin. As a main advantage, over the existing touch sensors, a single TE element can distinguish a different finger temperature, sense and discriminate between fast and slow touches, and give two symmetrical responses depending on the stimulated electrode, allowing for Yes–No/On–Off applications [11, 12, 29–33]. Among several desirable features, these devices must exhibit a strong sensing performance, including high and stable signal–noise ratio values with short response time. The chosen encapsulant materials, ethyl cellulose (EC) and PVA were deposited using blade-coating, while commercial plastic pouches were applied using an office laminator. The EC and PVA are flexible encapsulants and compatible with printed techniques, EC being cellulose-based is an eco-friendlier choice [34, 35], that to the best of our knowledge, it is used in this work for the first time as encapsulant for flexible electronic devices.

2 Materials and methods

2.1 TE samples preparation

A TE ink was formulated dissolving ethyl cellulose (CAS: 9004-57-3, Sigma-Aldrich, extent of labelling: 48% ethoxyl) in diacetone alcohol (DAA) (CAS: 123-42-2, 4-Hydroxy-4-methyl-2-pentanone 99% from Sigma-Aldrich) and adding 20 wt% of graphite flakes as received (mesh 325, 99.8%, metal basis from Alfa Aesar®). This ink was screen-printed (2 layers) with a mesh model 77-55, from I.C.M. Graf., Lda, using substrates of multi-function paper (office paper) with an 80 g m^{-2} grammage from The Navigator Company and natural cotton fabric from Fiacri. Carbon electrodes were then printed with a mesh model 120–34 and cured for 30 min at 100 °C, using a hot plate. To extend the device's electrical contacts, aluminium foils were glued on opposite sides of the quadrangular TE elements with screen-printed carbon electrodes. Further details can be found in a previous work [12].

2.2 Encapsulation step

The TE touch detectors were fully encapsulated (on both sides), as the substrates are fibrous, porous, and

susceptible to environmental changes equally and despite the side, and because a water submersion test was performed in order to validate an efficient encapsulation material. A representative schematic of the encapsulation and characterization processes can be found in Fig. 1.

Two encapsulant materials were deposited using blade-coating: a solution of 7.5 wt% EC dissolved in a mixture of 80:20 (V/V) of ethanol (EtOH) and DAA (EtOH, CAS: 64-17-5, from Carlo Erba Reagents), and a solution of PVA (CAS: 9002-89-5, from EVO-STIK) mixed with milli-Q water in a ratio of 1:7 (V/V). The blade coater used was a K101 Control Coater System, with a 4 µm or a 90 µm wet thickness rod or film applicator, correspondingly. The depositions were made with a bed temperature of 60 °C, at a speed level of 2 and 4 (these values do not have associated units according to the manufacturer equipment manual) for EC and PVA mixtures, respectively. Regarding EC encapsulation, after depositing one side and allowing it to dry for five minutes at 60 °C, the back was coated similarly. For the PVA samples, the back was coated after the first side had dried for 24 h at room temperature (RT). A commercial plastic pouch (thickness range of 80–125 µm) was also tested as an encapsulant using an OL 250-L-17 laminator from QUIGG, with a 400 mm/min operating speed, operating at a temperature of roughly 135 °C, according to the manufacturer.

2.3 Characterization

EC ink viscosity was measured using an Anto Paar Rheometer 502 TwineDrive, for shear rates from 1 to 1000 s^{-1}, at 25 and 60 °C. Thermogravimetric analysis (TGA) was conducted in a STA 449 F3 Jupiter, in air, with temperature varying from 25 to 500 °C at a heating ramp of 10 °C/min, to analyse the thermal properties of the selected encapsulant materials. Scanning electron microscope (SEM) Hitachi TM3030Plus tabletop workstation (Tokyo, Japan) was used for surface imaging, to see the differences between the substrates as purchased, after encapsulation and after the bending tests. Static water contact angle (CA) measurements were performed with DataPhysics OCA 15 Plus, using 2 µL droplets of deionized water. The side view of the droplet was acquired with a camera and the CA was determined using the Laplace-Young approximation model. A Gamry Instruments Reference 600 Potentiostat was used to measure the open circuit potential (V_{OC}) over time to determine the TE sensors' responsiveness to touch events, before and after the encapsulation step [11, 12]. These touch tests were conducted at room temperatures between 21.4 and 22.0 °C. Given that human fingertip temperatures at this ambient range typically fall between 30 and 32 °C [36], and that contact was made with a gloved finger for brief intervals, the actual temperature gradient observed across the sample itself was approximately 7–8 °C. Bending tests were conducted using a 15 mm curvature radius and water submersion tests were performed for 1 min, with the sensors being remeasured after.

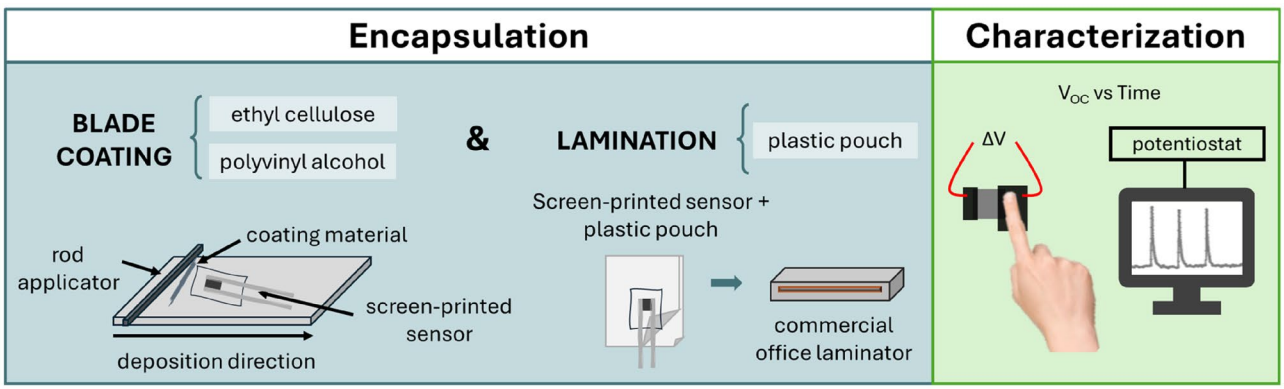

Fig. 1 An illustration of the two encapsulation techniques used, along with the corresponding materials, and the touch test employed in the characterization of the thermoelectric sensors

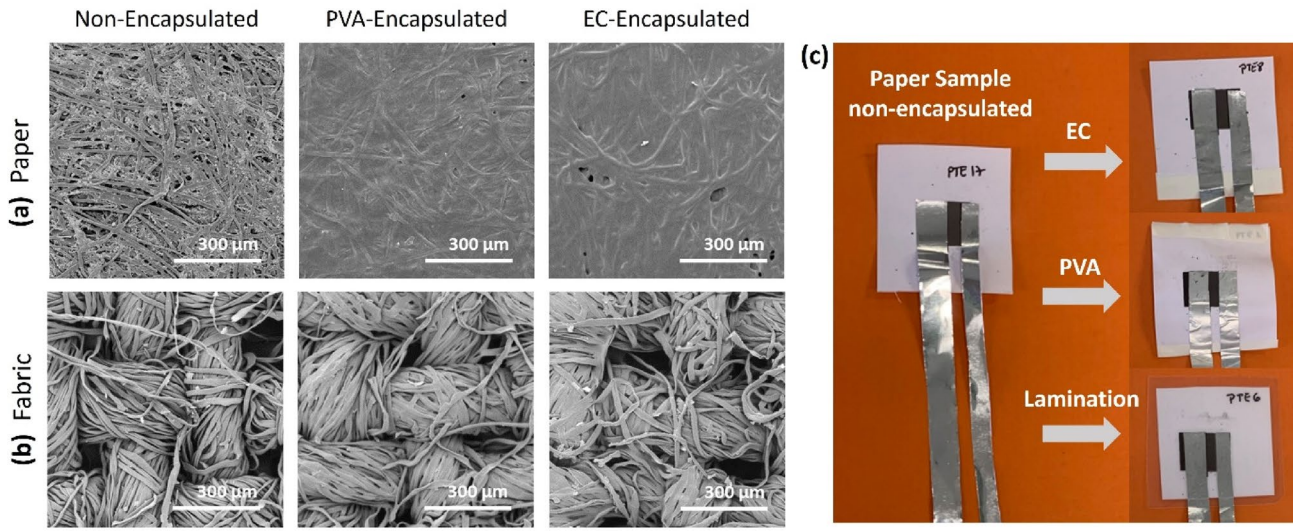

Fig. 2 SEM images for **a** paper samples and **b** fabric samples, before encapsulation, and after PVA and EC encapsulation; **c** Real images of the TE sensors, before and after the encapsulation with EC, PVA and plastic pouch lamination

3 Results and discussion

3.1 SEM imaging

SEM images in Fig. 2a and b reveal the differences between the two substrates used to print the TE sensors, before and after the PVA and EC encapsulation step. Both PVA and EC covered the paper surface uniformly, filling in the pores between the fibres and lining their walls. As for the fabric substrate, although the fibre threads seem to be covered, the gaps between them are relatively big to be filled with the encapsulant material, so the fabric remains porous. However, as published in a previous work regarding the TE sensors production [12], the TE ink itself helps to cover the substrates which will make the encapsulation more effective on top of an already printed paper or fabric.

Encapsulated and non-encapsulated samples subjected to bending tests were also analysed in areas with printed layers to determine whether any microfractures had formed. However, no visible differences were observed compared to the non-bent samples (Figure S 1 in the Supplementary Material). In Fig. 2c, we can confirm that both EC and PVA result in transparent encapsulation layers. A sample encapsulated with a laminated plastic pouch is also presented for comparison using conventional plastic encapsulant.

3.2 TGA analysis and viscosity

The TGA analysis of the three encapsulant materials and two substrate types studied in this work (Fig. S2—(a) in the Supplementary Material) demonstrates that all encapsulants are thermally stable up to150 °C. For applications requiring elevated processing or operational temperatures, a mass loss of 2% is observed at 162 °C, 276 °C and 381 °C, for PVA, EC and plastic lamination, respectively. Additionally, a mass loss of 10% is recorded at 307 °C, 315 °C and 408 °C, for PVA, EC and plastic lamination, respectively. Notably, PVA degrades more rapidly than EC, whereas plastic lamination is preferable at temperatures exceeding 250 °C, though at the expense of flexibility. For the substrates paper and fabric, an initial mass loss was observed below 100 °C, attributable to the desorption of free water within the fibres. Subsequently, at 295 °C for paper and 209 °C for fabric, a mass variation of approximately 10% occurred, corresponding to cellulose degradation [37, 38]. In contrast, the encapsulant materials demonstrate significant mass changes only at higher temperatures, indicating that the thermal degradation conditions affecting the substrates do not degrade the encapsulants.

Dynamic viscosity of commercial PVA is 9000–15000 mPa.s (depending on the dilution) according to the manufacturer's technical datasheet. The EC ink absolute viscosity measured

in the rheometer for a shear rate of 500 s^{-1} was 17.11 ± 0.02 mPa·s at 25 °C and 0.96 ± 0.08 mPa.s at 60 °C. These results (Figure S2—(b) in the Supplementary Material) show that both encapsulant inks are compatible and suitable for different printed techniques, such as screen-printing, dispenser-printing and blade coating, making the encapsulation process easily up-scalable [39, 40].

3.3 Contact angle

Contact angle (CA) measurements were performed to assess the wettability of the substrates both prior to and following encapsulation. The CA was also determined after subjecting the samples to 100 bending cycles with a 15 mm curvature radius. Additionally, the water resistance of the devices was tested by immersing them in water for 1 min. Prior to encapsulation, both paper and fabric exhibited high hydrophilicity, absorbing water droplets almost immediately, therefore, CA measurement was unfeasible as it fell below 10 degrees. This observation indicates that non-encapsulated sensors when wet or submerged in water, would likely experience a rapid degradation in electrical performance or potentially cease functioning. The CA values obtained are compiled in Fig. 3, showcasing the significant alterations in wettability resulting from each encapsulant material. The light-coloured bars represent measurements taken 1 min after the water droplet contacted the surface, while the darker bars refer to measurements taken at the 5 min mark.

Regarding the laminated samples, the CA values were comparable across both substrates, as anticipated. Unlike the other two encapsulation materials, the laminated plastic surface exhibited lower CA values after 5 min, attributed to evaporation and spreading of water on the low-energy surface. In the case of fabric samples encapsulated with PVA and EC, the CA values were higher compared to laminated plastic, indicating that, although the plastic surface is entirely impermeable to water, the EC and PVA encapsulants confer greater hydrophobicity to the surface, thus increasing the CA and sustaining it for longer. The EC mixture performed effectively on both substrates using a blade-coated layer applied with a 4 µm wet thickness rod. Although the PVA encapsulation on fabric yielded slightly higher CA values, the difference was negligible.

In contrast to the fabric samples, the PVA encapsulation (1:7 water ratio) with a single 4 µm rod passage was ineffective at creating a reliable water barrier on paper substrates, which completely absorbed the water droplet, resulting in a CA value near zero after 5 min. Due to the high dilution of PVA in water and despite the deposition being made at 60 °C, the paper fibres absorbed the solvent almost immediately, resulting in substantially lower performance of the PVA-encapsulated sensors on paper compared to those on fabric. To address this issue, different approaches were experimented. Initially, a 90 µm film applicator was utilized to increase PVA deposition and potentially enhance barrier performance. Additionally, a new PVA:water ratio (3:2 V/V) was tested, increasing the polymer in the mixture.

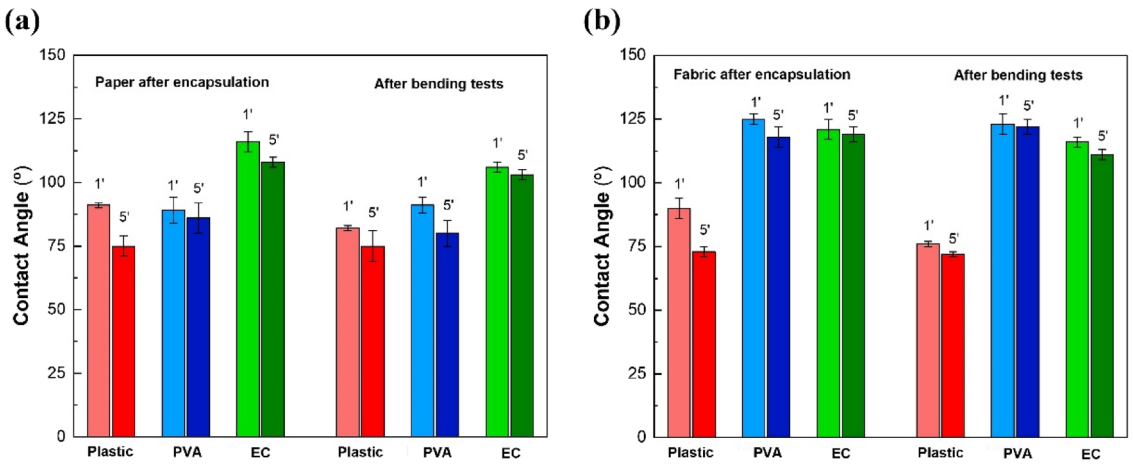

Fig. 3 Contact Angle values measured with three different encapsulants, after 1 and 5 min, for **a** paper samples and **b** cotton samples

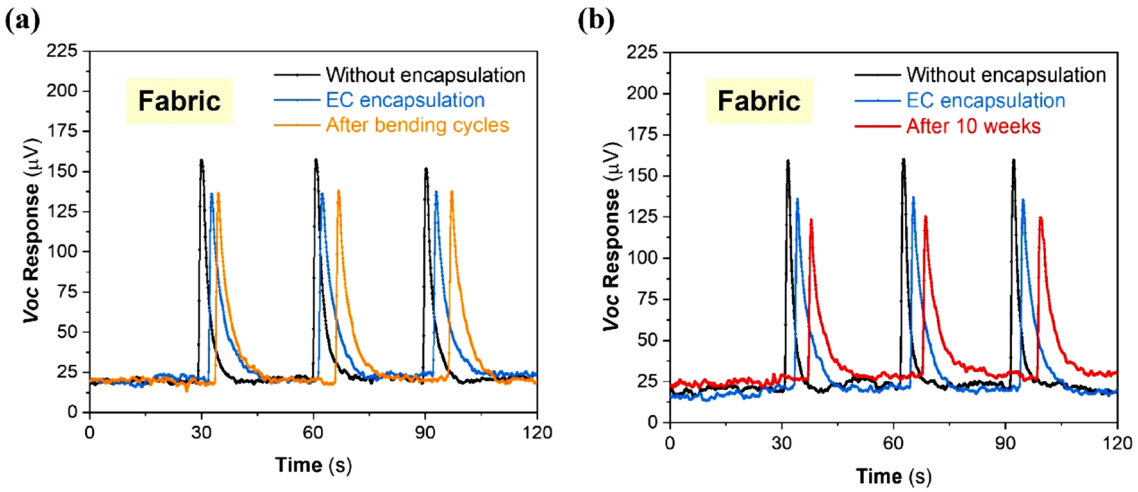

Fig. 4 Open circuit potential (V_{OC}) results for finger touch events. These cotton samples were characterized before and after the EC encapsulation, adding a characterization of an encapsulated sample: **a** after 100 bending tests and **b** after 10 weeks

However, neither approach yielded satisfactory results. The subsequent strategy involved increasing the number of printed layers while maintaining a 4 μm wet thickness per layer. This adjustment significantly improved the encapsulation of paper samples, leading to higher CA values and achieving a waterproof barrier, as confirmed by the manufacturer's datasheet (see Table S1 in the Supplementary Material). However, this modification significantly extended the encapsulation process due to the drying time required between layers and for each side of the sample. Although this approach enhanced the results, CA values remained approximately 30° lower for paper than for fabric samples across all tests. For EC encapsulation, the CA values were nearly identical for both substrates and demonstrated superior encapsulation efficiency in all test conditions, even following 1 min of water submersion (see Fig. 5b), affirming its anticipated hydrophobicity [41–43]. An additional contact angle measurement was conducted on EC and PVA-encapsulated samples before and after bending cycles, one year post-encapsulation, as shown in Figure S3. Results indicate that the values remain close to the previously measured values, with a variation of less than 10% in each case.

3.4 TE touch sensors

The V_{OC} of the TE sensors in response to gloved finger touches was measured over time. The V_{ON} represents the V_{OC} when the sample is experiencing a thermal gradient (ΔT) due to a finger touch in one of its electrodes, while V_{OFF} is considered the V_{OC} when no ΔT is applied between the electrodes. At the beginning of each test, the sample's response was recorded for at least 30 s without any touch events to establish a baseline. After this stabilization period, the sensors were stimulated, and the V_{OC} was allowed to return to its initial value before each subsequent touch event. The difference between the V_{ON} and V_{OFF} states is defined as the voltage amplitude (V_{AMP}) of the sensor's response [11, 12, 26].

This study prioritized the practical response of the TE sensors over conventional TE characterization. For touch-sensing applications, electrical resistance and conductivity are less critical than the Seebeck coefficient and the achievable thermal gradient across the sensor. Moreover, measuring thermal and electrical conductivities in these sensors on fibrous, porous substrates is challenging due to the indeterminate film thickness, while Seebeck measurements in samples with non-ideal dimensions contacts also face limitations. Consequently, our focus was on sensor functionality and stability in repeated touch tests under realistic conditions, rather than on calculating power factor or TE Figure of Merit. Non-encapsulated samples were tested before and after bending cycles, as shown in Figure S4, to establish a baseline for the typical behaviour of unencapsulated sensors.

The bending and submersion tests conducted with EC-encapsulated paper and fabric TE sensors Fig. 4

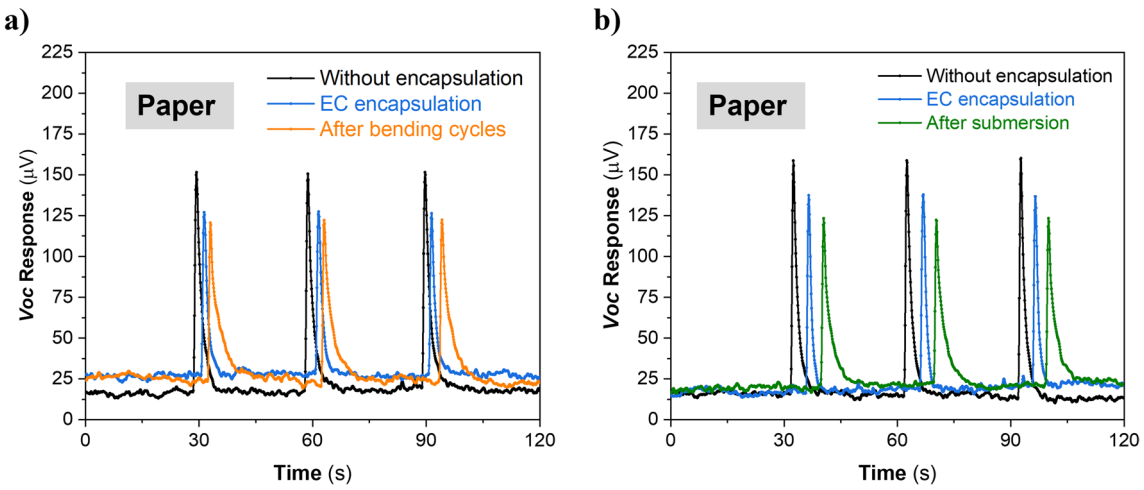

Fig. 5 Open circuit potential (V_{OC})results for finger touch events for paper samples that were characterized before and after the EC encapsulation, adding a characterization of an encapsulated sample: **a** after 100 bending tests and **b** after 1 min submersion

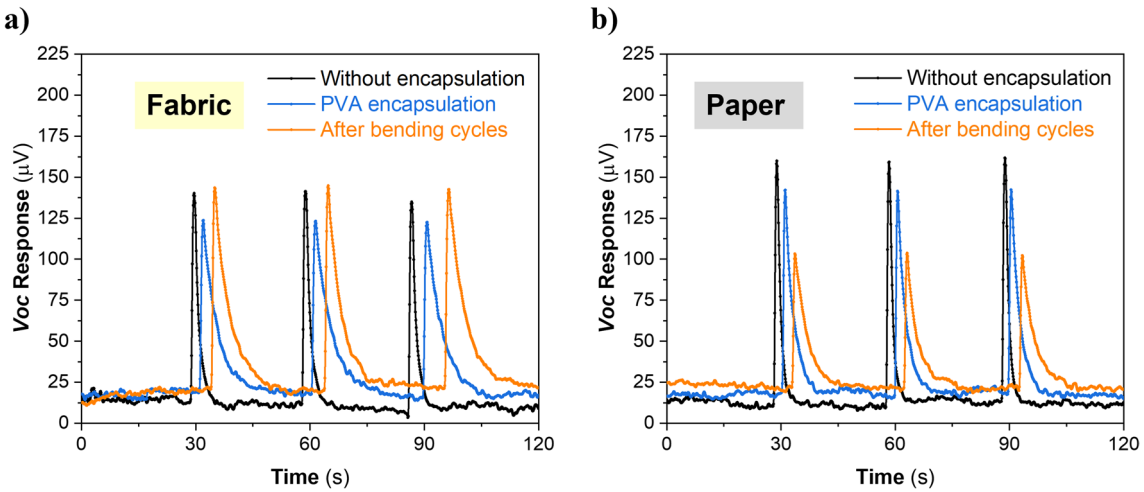

Fig. 6 Open circuit potential (V_{OC}) results for finger touch events. Both samples were characterized before and after the PVA encapsulation, and after the bending tests for: **a** encapsulated fabric sample and **b** encapsulated paper sample

and Fig. 5 demonstrate that the sensors remained functional even after 100 dynamic bending cycles with a 15 mm curvature radius or 1 min of water submersion. Although V_{AMP} values were slightly lower and off state recovery times (τ_{fall}) were prolonged, the response signal remained significant (~ 100 μV), and rise times maintained below 1 s. Results from the ageing tests, (Fig. 4b) indicate that, despite a reduction in V_{AMP} after 10 weeks, the EC-encapsulated device continued to function effectively. Similar ageing tests on PVA-encapsulated and laminated samples (see Figure S5—(a) and (b), respectively, in the Supplementary Material) showed that PVA-encapsulated sensors retained responsiveness, while laminated samples exhibited a significant decrease in V_{AMP} after 10 weeks.

In each plot, we observe that part of the V_{AMP} loss occurs immediately following the encapsulation step. This effect arises because an additional layer on the sensor hinders the thermal stimulus from reaching the electrode and slows heat dissipation after finger removal, thereby also increasing the τ_{fall}.

For fabric samples encapsulated with a single layer of PVA (Fig. 6a), the sensor performance after bending is comparable to that of EC encapsulation. However, for paper samples encapsulated with two PVA

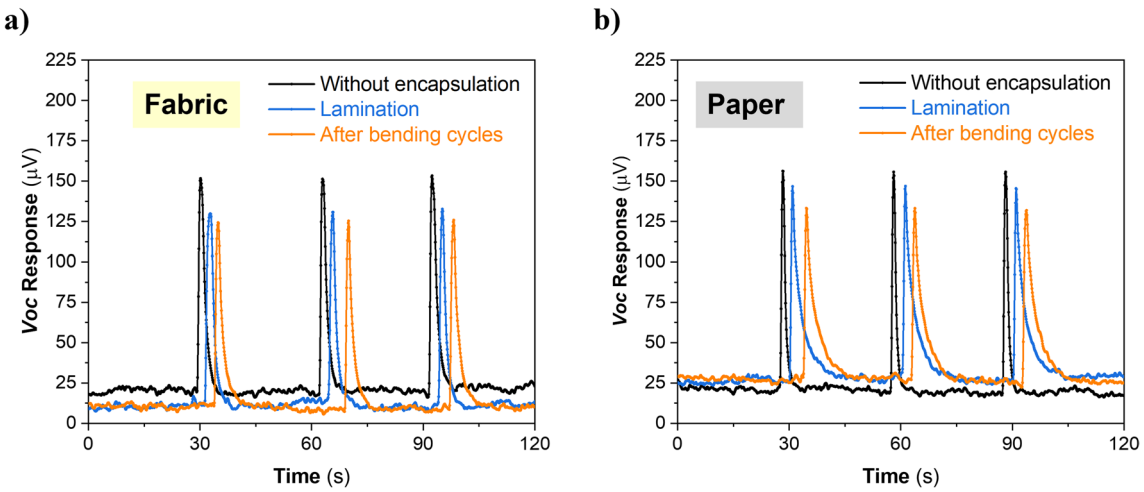

Fig. 7 Open circuit potential (V_{OC}) results for finger touch events. Both samples were characterized before and after the plastic lamination, and after the bending tests: **a** cotton sample and **b** paper sample

layers (see CA discussion in section C, which details the effect of varying PVA layers counts), the results reveal a significant decrease in V_{AMP} under bending stress for PVA-encapsulated sensors, Fig. 6b. Therefore, EC encapsulation is more suitable for flexible paper sensors, as it has a lesser impact on performance and involves a simpler, faster process.

For comparison purposes, fabric and paper samples encapsulated with laminated plastic were also evaluated using the same tests applied for EC and PVA, as shown in Fig. 7.

No improvement was observed with laminated plastic encapsulation for these TE sensors, as results indicated that the V_{AMP} continued to decrease, and response times also increased. For a detailed breakdown of V_{AMP} values, along with response and recovery times for all encapsulated fabric and paper samples, please refer to Tables S2 and S3 in the Supplementary Material. In terms of transparency, all the studied encapsulants were transparent, as shown in Fig. 2c. Additionally, due to the thicker plastic encapsulant layer, the samples appeared more rigid and heavier than those encapsulated with EC and PVA. This rigidity and added weight could be critical for applications where flexibility and low weight are key considerations.

4 Conclusion

In this study, we evaluated various encapsulants for flexible TE touch sensors printed on paper and fabric substrates, including ethyl cellulose and polyvinyl alcohol, applied via blade-coating, and laminated plastic using a commercial laminator. While laminated plastic provided a water-impermeable surface independently of the substrate, contact angle measurements indicated that both EC and the PVA significantly enhanced the waterproofing of previously non-encapsulated paper and fabric samples. Notably, following a 1 min water submersion test, the EC-encapsulated paper samples exhibited higher contact angles (103 ± 3º) than those encapsulated with PVA (87 ± 5º) or laminated plastic (84 ± 3º), underscoring EC's superior hydrophobicity. SEM surface imaging revealed that EC and PVA produced smoother, less porous surfaces on both paper and fabric substrates. Additionally, both laminated plastic and EC demonstrated thermal stability up to 200 °C, aligning well with the thermal demands flexible substrates in electronic applications. In terms of TE sensor performance, encapsulation introduced a decrease in V_{OC} and increased recovery times likely due to added thermal resistance. Nevertheless, all three encapsulants enabled effective touch detection, with response signals around 100 μV and rise times bellow 1 s. EC was identified as the optimal encapsulant due to its favourable electrical response, eco-friendly profile and compatibility with paper and on fabric substrates.

Moreover, EC's single-step blade coating application, requiring short drying times, supports scalability for large scale manufacturing. Given its tunable viscosity, EC encapsulants could also be applied via screen-printing or dispenser-printing, enhancing its versatility. This encapsulation material is thus well-suited not only for TE touch sensors but also for a broad range of printed and flexible electronic devices using diverse substrates.

Author contributions

The conception and design of this study were done by Joana Figueira, Cristina Gaspar and Emanuel Carlos. Material preparation, data collection and analysis were performed by Joana Figueira, Mariana Peixoto and Cristina Gaspar. The first draft of the manuscript was written by Joana Figueira, Mariana Peixoto, Cristina Gaspar and Emanuel Carlos and all authors commented on previous versions of the manuscript. All authors read and approved the final manuscript.

Funding

This work was financed by national funds from FCT—Fundação para a Ciência e a Tecnologia, I.P., in the scope of the projects LA/P/0037/2020, UIDP/50025/2020, and UIDB/50025/2020 of the Associate Laboratory Institute of Nanostructures, Nanomodelling and Nanofabrication—i3N, and projects 2022.04012.PTDC, and PTDC/CTM-PAM/4241/2020. J. Figueira thanks for the support from FCT through the PhD scholarship SFRH/BD/121679/2016. E. Carlos acknowledges funding received from FCT via 2021.03825.CEECIND. This work has received funding from the European Union's Horizon 2020 Research and Innovation Programme under Grant Agreements number 952169 (SYNERGY, H2020-WIDESPREAD-2020-5, CSA) and 101008701 (EMERGE, H2020-INFRAIA-2020-1), 101096021 (SUPERIOT, HORIZON-JU-SNS-2022-STREAM-B-01-03), and 101070255 (REFORM, HORIZON-CL4-2021-DIGITAL-EMERGING-01).

Data availability

The data supporting the findings of this study are available within the article and its supplementary information files. Any additional raw data that may be required are available from the corresponding author upon reasonable request.

Declarations

Competing interests The authors have no relevant financial or non-financial interests to disclose.

Supplementary Information The online version contains supplementary material available at https://doi.org/10.1007/s10854-024-14064-4.

Open Access This article is licensed under a Creative Commons Attribution-NonCommercial-NoDerivatives 4.0 International License, which permits any non-commercial use, sharing, distribution and reproduction in any medium or format, as long as you give appropriate credit to the original author(s) and the source, provide a link to the Creative Commons licence, and indicate if you modified the licensed material. You do not have permission under this licence to share adapted material derived from this article or parts of it. The images or other third party material in this article are included in the article's Creative Commons licence, unless indicated otherwise in a credit line to the material. If material is not included in the article's Creative Commons licence and your intended use is not permitted by statutory regulation or exceeds the permitted use, you will need to obtain permission directly from the copyright holder. To view a copy of this licence, visit http://creativecommons.org/licenses/by-nc-nd/4.0/.

References

1. M.L. Seol et al., Printing of a passivation layer for the protection of printed supercapacitors. ACS Appl. Electron. Mater. **2**(11), 3643–3649 (2020)

2. J. Figueira et al., Sustainable fully printed UV sensors on cork using zinc oxide/ethylcellulose Inks. Micromachines **10**(9), 1–10 (2019)
3. C. Gaspar, J. Olkkonen, S. Passoja, M. Smolander, Paper as active layer in inkjet-printed capacitive humidity sensors. Sensors **17**(1464), 1–10 (2017)
4. L.P.R. Barras, I. Cunha, D. Gaspar, E. Fortunato, R. Martins et al., Printable cellulose-based electroconductive composites for sensing elements in paper electronics. Flex. Print. Electron. **2**, 1–12 (2017)
5. N.M. Nair, I. Khanra, D. Ray, P. Swaminathan, Silver nanowire-based printable electrothermochromic Ink for flexible touch-display applications. ACS Appl. Mater. Interfaces **13**(29), 34550–34560 (2021)
6. A.K. Jaiswal, A. Hokkanen, V. Kumar, T. Mäkelä, A. Harlin, H. Orelma, Thermoresponsive nanocellulose films as an optical modulation device: proof-of-concept. ACS Appl. Mater. Interfaces **13**, 25346–25356 (2021)
7. P. Pathak, S. Park, H.J. Cho, A carbon nanotube-metal oxide hybrid material for visible-blind flexible UV-Sensor. Micromachines **11**, 368 (2020)
8. S. Smocot, Z. Zhang, L. Zhang, S. Guo, C. Cao, Printed flexible mechanical sensors. Nanoscale **14**(46), 17134–17156 (2022)
9. Q. Liu et al., All textile-based robust pressure sensors for smart garments. Chem. Eng. J. **454**(P2), 140302 (2023)
10. S. Ahmad, K. Rahman, M. Shakeel, T.A.K. Qasuria, T.A. Cheema, A. Khan, A low-cost printed humidity sensor on cellulose substrate by EHD printing. J. Mater. Res. **36**(18), 3667–3678 (2021)
11. J. Figueira, J. Loureiro, E. Vieira, E. Fortunato, R. Martins, L. Pereira, Flexible, scalable, and efficient thermoelectric touch detector based on PDMS and graphite flakes. Flex. Print. Electron. **6**, 045018 (2021)
12. J. Figueira et al., Screen-printed, flexible, and eco-friendly thermoelectric touch sensors based on ethyl cellulose and graphite flakes inks. Flex. Print. Electron. **8**, 025001 (2023)
13. B.A. Kuzubasoglu, E. Sayar, C. Cochrane, V. Koncar, S.K. Bahadir, Wearable temperature sensor for human body temperature detection. J. Mater. Sci. Mater. Electron. **32**(4), 4784–4797 (2021)
14. S. Tachibana et al., Flexible printed temperature sensor with high humidity stability using bilayer passivation. Flex. Print. Electron. **6**(3), 034002 (2021)
15. T. Kinkeldei, N. Munzenrieder, C. Zysset, K. Cherenack, G. Tröster, Encapsulation for flexible electronic devices. IEEE Electron Device Lett. **32**(12), 1743–1745 (2011)
16. Z. Cui, *Printed electronics: materials technologies and applications* (Wiley, Hoboken, 2016)
17. Y. Li, S. Arumugam, C. Krishnan, M.D.B. Charlton, Encapsulated textile organic solar cells fabricated by spray coating. ChemistrySelect **4**, 407–412 (2019)
18. F. Brunetti et al., Printed solar cells and energy storage devices on paper substrates. Adv. Funct. Mater. (2019). https://doi.org/10.1002/adfm.201806798
19. J.C. Zhu et al., A flexible micro direct methanol fuel cells array based on FPCB. Energy Convers. Manag. **258**, 115469 (2022)
20. N. Jiang et al., Ionic liquid enabled flexible transparent polydimethylsiloxane sensors for both strain and temperature sensing. Adv. Compos. Hybrid Mater. **4**(3), 574–583 (2021)
21. Z. Fan, Y. Zhang, L. Pan, J. Ouyang, Q. Zhang, Recent developments in flexible thermoelectrics: from materials to devices. Renew. Sustain. Energy Rev. **137**, 110448 (2020)
22. Z. Li et al., Efficient strain modulation of 2D materials via polymer encapsulation. Nat. Commun. **11**(1), 1–8 (2020)
23. Q. Zhang, Y. Di, C.M. Huard, L.J. Guo, J. Wei, J. Guo, Highly stable and stretchable graphene-polymer processed silver nanowires hybrid electrodes for flexible displays. J. Mater. Chem. C **3**(7), 1528–1536 (2015)
24. A.R. Correia, *Tailoring carbon-based materials for thermoelectric application* (University of Porto, Porto, 2019)
25. Y. Du, H. Li, X. Jia, Y. Dou, J. Xu, P. Eklund, Preparation and thermoelectric properties of graphite/poly(3,4-ethyenedioxythiophene) nanocomposites. Energies **11**, 2849 (2018)
26. J. Figueira et al., Composites based on PDMS and graphite flakes for thermoelectric sensing applications. Mater. Proc. **8**, 42 (2022)
27. S. Duan et al., Printable graphite-based thermoelectric foam for flexible thermoelectric devices. Appl. Phys. Lett. (2023). https://doi.org/10.1063/5.0159347
28. Q. Liu et al., Cheap, large-scale, and high-performance graphite-based flexible thermoelectric materials and devices with supernormal industry feasibility. ACS Appl. Mater. Interfaces **14**(6), 8066–8075 (2022)
29. J. Figueira, *Printed Eco-materials for flexible thermoelectric devices* (NOVA University Lisbon, Lisbon, 2023)
30. E.M.F. Vieira et al., Highly sensitive thermoelectric touch sensor based on p-type SnO x thin film. Nanotechnology **30**, 43 (2019)
31. E.M.F. Vieira et al., Enhanced thermoelectric properties of Sb2Te3 and Bi_2Te_3 films for flexible thermal sensors. J. Alloys Compd. **774**, 1102–1116 (2019)
32. M. Ruoho, T. Juntunen, T. Alasaarela, M. Pudas, I. Tittonen, Transparent flexible and passive thermal touch panel. Mater. Technol. Adv. (2016). https://doi.org/10.1002/admt.201600204

33. J. Figueira et al., Optimization of cuprous oxides thin films to be used as thermoelectric touch detectors. ACS Appl. Mater. Interfaces **9**(7), 6520–6529 (2017)
34. H. Seddiqi et al., Cellulose and its derivatives: towards biomedical applications. Cellulose **28**(4), 1893–1931 (2021)
35. Y. Lu, Y. Wang, L. Liu, W. Yuan, Environmental-friendly and magnetic/silanized ethyl cellulose sponges as effective and recyclable oil-absorption materials. Carbohydr. Polym. **173**, 422–430 (2017)
36. E.F.J. Ring, K. Ammer, Infrared thermal imaging in medicine. Physiol. Meas. **33**, R33 (2012)
37. D. Gaspar, *Active cellulose-based substrates for application in electronic devices, school of science and technology* (NOVA University Lisbon, Lisbon, 2019)
38. J.T. Carvalho, *Sustainable fiber-based structures for application in electronic and electrochemical systems* (NOVA University Lisbon, Lisbon, 2023)
39. T. Öhlund, *Metal films for printed electronics : Ink-substrate interactions and sintering* (Mid Sweden University, Östersund, 2014)
40. Z. Cao, *Printable Thermoelectric devices for energy harvesting* (University of Southampton, Southampton, 2014)
41. T.A. Ahmed, M.A.A. Suhail, K.M. Hosny, F.I. Abd-Allah, Clinical pharmacokinetic study for the effect of glimepiride matrix tablets developed by quality by design concept. Drug Dev. Ind. Pharm. **44**(1), 66–81 (2018)
42. G. Kimbell, M.A. Azad, 3D printing: bioinspired materials for drug delivery, in *Bioinspired and biomimetic materials for drug delivery*. (Elsevier, Cham, 2021), pp.295–318
43. R. Sharma et al., Recent advances in cellulose-based sustainable materials for wastewater treatment: an overview. Int. J. Biol. Macromol. **256**, 128517 (2024)

Publisher's Note Springer Nature remains neutral with regard to jurisdictional claims in published maps and institutional affiliations.